The structure and spectroscopy of lanthanide(III) complexes with 2,2′-bipyridine-1,1′-dioxide in solution and in the solid state: effects of ionic size and solvent on photophysics, ligand structure and coordination†

Ewa Huskowska,[a] Ilona Turowska-Tyrk,[b] Janina Legendziewicz*[a] and James P. Riehl[c]

[a] *Faculty of Chemistry, University of Wrocław, Joliot-Curie 14, 50-383, Wrocław, Poland. E-mail: jl@wchuwr.chem.uni.wroc.pl*
[b] *Institute of Physical and Theoretical Chemistry, Wrocław University of Technology, Wybrzeże Wyspianskiego 27, 50-370, Wrocław, Poland*
[c] *Department of Chemistry, University of Minnesota Duluth, Duluth, Minnesota 55812, USA*

Received (in Montpellier, France) 18th February 2002, Accepted 13th May 2002
First published as an Advance Article on the web 16th August 2002

Single crystals of [Ln(2,2′-bipyridine-1,1′-dioxide)$_4$](ClO$_4$)$_3$ (Ln = Nd, Lu) have been obtained and the crystal structures determined. By comparison with previous structural determinations, it is demonstrated that steric crowding associated with the decreasing lanthanide ions radius causes changes of the angles between the rings of the ligand. This leads to a deformation of the coordination polyhedron from an almost ideal cube (La, Ce) to a dodecahedron distorted towards a square antiprism (for Nd and heavier lanthanides), and slightly distorted square antiprism for Lu. Electronic absorption spectra of Nd(bpyO$_2$)$_4^{3+}$ and Eu(bpyO$_2$)$_4^{3+}$ (bpyO$_2$ = 2,2′-bipyridine-1,1′-dioxide) at room temperature and 4 K were measured in CH_3CN and CH_3NO_2 and in the solid state. Emission and excitation spectra, and lifetime measurements of Tb(bpyO$_2$)$_4^{3+}$ at 293 and 77 K are presented and used to characterize the excited state photophysics of this species. Comparisons are made to previous results, and generalizations concerning molecular and electronic structure for the series of complexes are presented.

1. Introduction

The design of efficient luminescence materials and compounds based on lanthanide(III) complexes remains an area of active investigation. Although lanthanide complexes with both acyclic and macrocyclic ligands are being studied, for a variety of electronic and structural reasons, complexes with large macrocyclic ligand systems are finding increased interest and applications. For example, a considerable amount of recent work has been devoted to the luminescence properties of lanthanide(III) complexes involving Eu(III) and Tb(III) with cryptates containing heterocyclic components, which are known to efficiently encapsulate the lanthanide ion. These types of complexes are known to form relatively stable structures that in some cases are well protected from penetration of the inner coordination sphere by solvent molecules and counter ions. Heterocyclic ligands, especially the derivatives bearing N-oxide functions, may be particularly stable, and are often efficient sensitizers for lanthanide ion emission upon UV irradiation. For these reasons and others, complexes such as these may be good candidates for exploitation as time-resolved fluoroimmunoassay agents.[1–9]

There have been a number of recent spectroscopic investigations involving the complexation of lanthanide(III) ions with ligands containing 2,2′-bipyridine-1,1′-dioxide (bpyO$_2$) and related species.[1–9] Most of these studies were concerned with the structure, stability, photophysics, or dynamics of the complexes under study. Experimental and theoretical results for the quantum yield of 4f → 4f emission have also been reported.[2,4,6,10] In our laboratory we have used circularly polarized luminescence spectroscopy (CPL) following circularly polarized excitation of Eu(bpyO$_2$)$_4^{3+}$ in acetonitrile solution to probe the chiral solution structure of this species.[1] In addition, theoretical and experimental studies concerned with the mechanism of excited state energy transfer in solid Eu(bpyO$_2$)$_4$(ClO$_4$)$_3$ have also been performed.[4] Of continued interest and importance are the solution dynamics, stereochemical lability, and the role of solvent in the solution structure and excited state dynamics of these classes of complexes. The type of information obtained is of obvious importance in the design of macrocyclic species in which bpyO$_2$ and similar N-oxide heterocycles are a constituent.

In this work we present high-resolution absorption and emission spectra for complexes of Nd(III), Eu(III), and Tb(III) with bpyO$_2$ in the solid state and in solution media. The results are interpreted in terms of important structural and electronic properties. We also report the results of X-ray diffraction measurements for a series of Ln(bpyO$_2$)$_4$(ClO$_4$)$_3$ compounds, in order to study the effect of steric crowding associated with the decrease of the lanthanide ionic radius. These structural studies are of special interest, since, to date, only a very small number of crystallographic data describing monomeric lanthanide complexes with coordination number 8 in which the coordination polyhedron is a cube have appeared in the literature.[11,12]

† Electronic supplementary information (ESI) available: ORTEP drawings of Nd(bpyO$_2$)$_4^{3+}$, Lu(bpyO$_2$)$_4^{3+}$ and perchlorate anions in Nd crystal structure; absorption spectra of Nd(bpyO$_2$)$_4^{3+}$. See http://www.rsc.org/suppdata/nj/b2/b201846m/

2. Experimental

Crystals of $Nd(bpyO_2)_4(ClO_4)_3$ and $Lu(bpyO_2)_4(ClO_4)_3$ were grown either using the method of Miller and Madan[13] as described in ref. 1, or by allowing an aqueous solution containing a 1:4 ratio of Ln(III) and $bpyO_2$ to evaporate slowly. Anhydrous perchlorates of Nd(III), Eu(III) and Tb(III) were prepared from $Ln(ClO_4)_3 \cdot nH_2O$ according to the previously described dehydration procedure.[14,15]

Crystal structures

Crystals of $[Ln(2,2'\text{-bipyridine-}1,1'\text{-dioxide})_4](ClO_4)_3$ (Ln = Nd, Lu) were examined on a Kuma KM4CCD diffractometer equipped with a CCD camera. The general strategy of data collections used for area-detector diffractometers was described elsevere.[16] Precise cell constants were determined by the least-squares method using most of the measured reflections. The data were corrected for the Lorentz-polarization effects.[17]

Both structures were solved by direct methods from SHELXS86 program.[18] For the Nd crystal most of the non-hydrogen atoms were detected, but for the Lu complex only a fraction were revealed; the remaining atoms were found by several difference Fourier syntheses. The Nd and Lu structures were refined by SHELXL93[19] and SHELXL97,[20] respectively. In both cases all non-hydrogen atoms were treated anisotropically and hydrogens were refined with constraints. In contrast to the Nd compound that was examined in which there are no water molecules in the crystal, in the Lu structure there are two water molecules per one lanthanide complex. H atoms in the water molecules were not seen clearly, and thus were not included in the Lu structure model. In the Nd crystal two of three ClO_4^- anions are seriously disordered. The disorder was described as a superposition of two equal orientations for which some geometrical restraints (DFIX possibility from SHELXL93) were applied. In the case of the Lu derivative for atoms in the $bpyO_2$ rings some restraints were also applied (ISOR, SIMU and DFIX from SHELXL97). For the Lu structure one electron density maximum (of height 2.76 e $Å^{-3}$) in the final ΔF map could not be interpreted. This maximum is situated about 1.6 Å from N4 and 2.1 Å from N6 and gives nearly a tetrahedral coordination around both N atoms and almost linear contacts to them. Excluding this maximum, $\rho_{max} = 1.07$ e $Å^{-3}$ and $\rho_{min} = -1.04$ e $Å^{-3}$, close to ClO_4^- and to Lu, respectively. The final Flack parameter for the Lu crystal was −0.001(15) which additionally confirmed the choice of the acentric space group (besides statistics of intensities) and the proper determination of the absolute structure.[21]

The crystal size for the Nd complex was $0.30 \times 0.30 \times 0.28$ mm^3. We collected the X-ray data by the area detector (CCD camera). Due to the strategy of the data collection, intensities of the same reflection were measured for different crystal orientations and afterwards were averaged. Such a procedure concerned many reflections. The crystal shape and the data collection strategy were the main reasons that we did not applied absorption corrections for the Nd complex. For the Lu derivative we used the same strategy of data collection as for the Nd complex. The crystal size for the Lu derivative was $0.08 \times 0.08 \times 0.04$ mm^3. Since we observed one uninterpreted maximum in the structure, we tried absorption corrections. Unfortunately, they did not change the residual electron density. The maximum mentioned above did not become smaller and thermal ellipsoids were not improved.

CCDC reference numbers 178801 and 178802. See http://www.rsc.org/suppdata/nj/b2/b201846m/ for crystallographic data in CIF or other electronic format.

Spectroscopic measurements

Electronic absorption spectra of Nd and Eu complexes in acetonitrile and nitromethane and in the solid state were recorded on a Cary-Varian 500 spectrophotometer equipped with a helium flow cryostat (OXFORD CF 1204) in the region 300–1000 nm. The intensities of the $f \leftrightarrow f$ transitions were calculated by integration of the Gauss–Lorentzian curve and transformed to oscillator strength values using the ICH 10 program. The details of the intensity, τ_λ and Ω_λ, parameter calculations were described in the paper.[22] The high-resolution excitation and emission spectra were recorded at 293, 77 and 4 K using a Spectra Pro 0.75-m monochromator equipped with a Hamamatsu R928 photomultiplier tube as a detector and an Oxford 1024 continuous flow helium cryostat. Luminescence decay times were measured using a Jobin-Yvon THR 1000 monochromator and Lambda-Physik 105 excimer laser.

3. Results and discussion

Crystallographic results

The crystal structure data and refinement details for $[Ln(2,2'\text{-bipyridine-}1,1'\text{-dioxide})_4](ClO_4)_3$ (Ln = Nd, Lu) are given in Table 1. Selected bond lengths and bond angles are listed in Table 2. ORTEP plots of the structures of the neodymium and lutetium complexes are given as electronic supplementary information (ESI†). In both structures the Ln(III) ions are coordinated by eight oxygen atoms from four $bpyO_2$ ligands. The Ln–O coordination bond lengths varies from 2.386(4) to 2.495(4) Å and 2.276(7) to 2.334 (8) Å for Nd and Lu, respectively (Table 2). The coordination polyhedron can be described as a dodecahedron (Dod) smoothly distorted towards square antiprism (SAP) for the neodymium complex. For this complex the symmetry deviation parameter Δ, defined as the mean square distance between the observed and ideal positions of the atoms in the dodecahedron, is 0.0355 $Å^2$, whereas for SAP Δ is equal to 0.143 $Å^2$. In the Dod structure the characteristic angles θ_A and θ_B, defined as the angles between the M–O bonds and the S_4 axis, are equal to 45.8 and 63.2° (for the ideal Dod these angles should be 36.9 and 69.5°, respectively). The characteristic structural parameter for the square antiprism is the angle θ between the M–O bond and the S_8 axis. For the ideal SAP, θ is equal to 59.2°, whereas the corresponding

Table 1 Crystallographic details

Molecule	$[Nd(bpyO_2)_4](ClO_4)_3$	$[Lu(bpyO_2)_4](ClO_4)_3 \cdot 2H_2O$
Chemical formula	$C_{40}H_{32}Cl_3N_8NdO_{20}$	$C_{40}H_{36}Cl_3N_8LuO_{22}$
Formula weight	1195.33	1262.09
Crystal system	Monoclinic	Orthorhombic
a/Å	14.8396(8)	14.2770(10)
b/Å	13.5620(8)	23.8122(18)
c/Å	23.0193(14)	13.4358(11)
β/deg	91.405(5)	
V/$Å^3$	4631.3(5)	4567.7(6)
Z	4	4
Space group	$P2_1/c$	$Pna2_1$
Temp./K	293(2)	100(2)
μ/mm^{-1}	1.38	2.43
Number of collected reflections	26 565	27 264
Number of independent reflections	9072	6436
Number of observed ind. reflections	7354	5317
R_{int}	0.035	0.067
Final R indices $[I > 2\sigma(I)]$	$R_1 = 0.061$, $wR_2 = 0.129$	$R_1 = 0.061$, $wR_2 = 0.107$
Final R indices (all data)	$R_1 = 0.074$, $wR_2 = 0.133$	$R_1 = 0.081$, $wR_2 = 0.113$

Table 2 Selected bond lengths/Å and bond angles/deg

Bond	$[Nd(bpyO_2)_4](ClO_4)_3$	$[Lu(bpyO_2)_4](ClO_4)_3{\cdot}2H_2O$
Ln–O(1)	2.490(4)	2.310(7)
Ln–O(2)	2.386(4)	2.314(9)
Ln–O(3)	2.451(4)	2.276(7)
Ln–O(4)	2.432(4)	2.313(8)
Ln–O(5)	2.433(4)	2.319(8)
Ln–O(6)	2.431(4)	2.334(8)
Ln–O(7)	2.394(4)	2.313(7)
Ln–O(8)	2.495(4)	2.308(8)
Angle	**$[Nd(bpyO_2)_4](ClO_4)_3$**	**$[Lu(bpyO_2)_4](ClO_4)_3{\cdot}2H_2O$**
O(2)–Ln–O(1)	68.5(2)	71.2(3)
O(3)–Ln–O(1)	127.6(2)	154.5(3)
O(4)–Ln–O(1)	72.53(14)	89.2(3)
O(5)–Ln–O(1)	91.85(14)	73.2(2)
O(6)–Ln–O(1)	158.4(2)	133.4(3)
O(7)–Ln–O(1)	72.6(2)	108.9(2)
O(8)–Ln–O(1)	112.75(14)	71.9(3)
O(3)–Ln–O(2)	162.1(2)	86.9(3)
O(4)–Ln–O(2)	126.3(2)	75.7(3)
O(5)–Ln–O(2)	74.2(2)	131.0(3)
O(6)–Ln–O(2)	94.8(2)	154.7(2)
O(7)–Ln–O(2)	106.3(2)	72.4(3)
O(8)–Ln–O(2)	72.0(2)	115.3(3)
O(4)–Ln–O(3)	70.4(2)	72.6(3)
O(5)–Ln–O(3)	109.7(2)	115.4(2)
O(6)–Ln–O(3)	71.3(2)	70.3(3)
O(7)–Ln–O(3)	75.4(2)	74.9(2)
O(8)–Ln–O(3)	92.7(2)	131.1(3)
O(5)–Ln–O(4)	71.5(2)	71.3(3)
O(6)–Ln–O(4)	110.3(2)	106.2(3)
O(7)–Ln–O(4)	95.5(2)	135.1(3)
O(8)–Ln–O(4)	160.0(2)	151.9(3)
O(6)–Ln–O(5)	69.83(14)	71.0(3)
O(7)–Ln–O(5)	162.44(14)	152.6(3)
O(8)–Ln–O(5)	125.9(2)	83.2(3)
O(7)–Ln–O(6)	127.0(2)	90.8(3)
O(8)–Ln–O(6)	72.3(2)	75.2(3)
O(8)–Ln–O(7)	69.2(2)	72.1(3)

angle in a cube is 54.1°.[23] In the lutetium complex the coordination polyhedron is a slightly deformed square antiprism ($\Delta = 0.055$ Å^2, $\theta = 55.4°$).

In the $La(bpyO_2)_4(ClO_4)_3$ cluster in the structure reported by Al-Karaghouli *et al.*,[11] the metal ion is also coordinated by eight oxygen atoms as in the neodymium and lutetium complexes. However, there are some differences between the structures caused by the decreasing ionic radius across the lanthanide series and increased repulsion between oxygen atoms of the ligands. Ionic radii for the lanthanide ions with a coordination number 8 are equal to 1.160 Å (La), 1.143 Å (Ce), 1.126 Å (Pr), 1.109 Å (Nd), 1.066 Å (Eu), 1.040 Å (Tb), 0.985 Å (Yb) and 0.977 Å (Lu).[24] The distortion of angles transforms a cube to a dodecahedron and a square antiprism. This corresponds to a point symmetry change from $O_h \rightarrow D_{2d} \rightarrow D_{4d}$. A pathway from the Dod to the SAP exists through an intermediate structure with D_2 symmetry.[23] For the largest ion, *i.e.* La^{3+}, the steric crowding is less than that for the other lanthanides. The lanthanum ion is located on a two-fold axis and crystallizes in the *Pbcn* space group.[11] In this structure, the angles between the planes of the rings are almost identical for the four ligands (mean value equals 61.4°), and the La–O distances are also very similar (2.495–2.512 Å). These factors make possible the creation of a coordination polyhedron with high symmetry (slightly distorted cube) with a mean value of θ equal to 56.1°. The cerium complex is isostructural with $La(bpyO_2)_4(ClO_4)_3$.[25] Since the spectroscopic properties (absorption and emission) of this ion are different in nature, they will be the subject of a forthcoming paper together with data of the corresponding Yb(III) compound.[25] It is worth noting that the cube is a rare coordination polyhedron for lanthanide ions. It has been observed mainly for complexes with unidentate ligands such as in La(pyridine-*N*-oxide)$_8(ClO_4)_3$.[12]

There is only a very small decrease in ionic radius in going from Ce^{3+} and Pr^{3+} to Nd^{3+} (1.143–1.109Å.[24]) This change, and the associated steric crowding, is apparently of sufficient magnitude, however, to affect the angle between the rings in the individual ligands. For Nd^{3+} ion the angles are 57.7°, 65.9°, 61.6°, and 57.7°. Accompanying this change is a change in coordination polyhedron from a cube to a slightly deformed dodecahedron. The space group for the praseodymium and neodymium complexes is $P2_1/c$, also different from that seen for the lanthanum complex (*Pbcn*).

The decrease of ionic radius to 1.066 Å for Eu^{3+} provides further changes in the crystal structure of this complex. As reported previously,[4] the Eu(III) species crystallizes in the $P2_1$ space group [$a = 14.730(1)$, $b = 13.585(1)$, $c = 22.967(2)$ Å, $\beta = 91.46(1)°$] with two crystallographically distinct metal ions. In this case, the increased steric crowding and ligand repulsion forces cause larger twists of the ligand ring systems. Angles of 55.1 to 68.3° are observed for Eu(1) and 55.3 to 65.9° are seen for Eu(2). The coordination polyhedra are dodecahedral, but are now more distorted towards SAP than in the case of the neodymium complex. Preliminary data for $Ho(bpyO_2)_4(ClO_4)_3$ [$a = 14.73(14)$, $b = 13.61(9)$, $c = 22.80(10)$ Å, $\beta = 92.6(5)°$] indicate that it is isostructural with the corresponding europium complex.

Further deformation of the cubic system and twisting of the planes of the ligand rings leads to a polyhedron which can be described as a slightly distorted square antiprism. This is what is observed for the Lu complex. The angles between the planes of $bpyO_2$ rings are in this case equal to 52.0(3), 57.3(3), 58.8(3), and 57.9(2)°. Transformation of the cubic system towards the square antiprism does not require differentiation of Lu–O bond lengths (see Table 2). This change is accompanied by a change in space group to orthorhombic $Pna2_1$ with cell constants $a = 14.2770(10)$, $b = 23.8122(18)$ Å and $c = 13.4358(11)$. Transformation of the cubic system through dodecahedral to antiprismatic is shown in Fig. 1.

These results illustrate the caution that one must take in extending the results obtained for one complex to the rest of the lanthanide series. As demonstrated, complexes of lanthanide ions with the same ligand through the series may preserve the same atomic coordination, but need not be isomorphic, and may, in fact, be associated with different coordination polyhedra and symmetry of Ln(III) ions.

Spectroscopic results

The absorption spectra of $Nd(bpyO_2)_4(ClO_4)_3$ dissolved in CH_3CN and CH_3NO_2 are provided as electronic supplementary information,† and the absorption spectra of this compound in the solid state at 300 K and 4 K are shown in

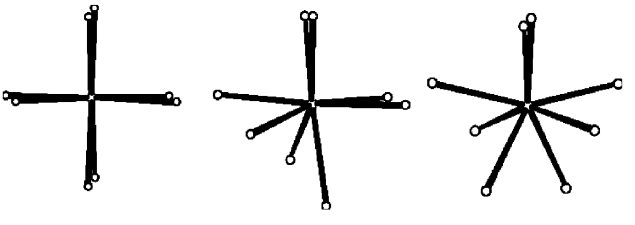

Fig. 1 Transformation of the cubic system [La(III)] through dodecahedral [Nd(III)] to antiprismatic [Lu(III)].

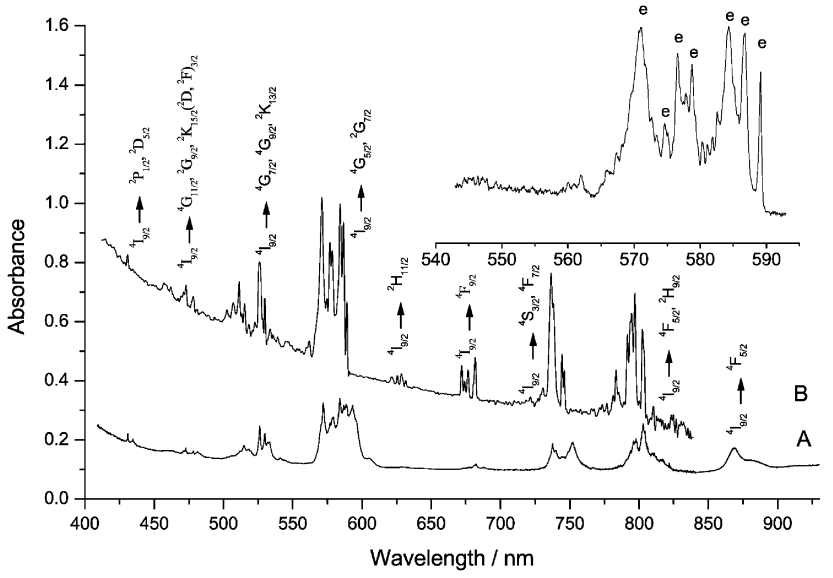

Fig. 2 Absorption spectra of $Nd(bpyO_2)_4(ClO_4)_3$ crystals at room temperature (A) and 4 K (B) (e = electronic line, the rest = vibronic components).

Fig. 2. Comparative emission excitation spectra for the corresponding Tb(III) and Eu(III) complexes in the UV region are plotted in Fig. 3. As seen in these figures, the absorption spectra in the UV region are dominated by electronic transitions involving the $bpyO_2$ ligands. It should be noted, however, that the spectrum for the $Eu(bpyO_2)_4^{3+}$ species displayed in Fig. 3, also shows the presence of a charge transfer (CT) transition centered at approximately 370 nm. The relative location of the CT transition has important consequences in terms of the efficiency of lanthanide ion luminescence.[2,6,26]

The absorption spectrum of neodymium systems in the visible and near-IR region involves parity forbidden $f \rightarrow f$ transitions from the $^4I_{9/2}$ ground state multiplet to various excited states. The integrated intensities of these transitions have been analyzed in terms of Judd–Ofelt theory[27,28] and are presented in Table 3 in units of oscillator strength. The details of the f–f transition intensity calculations were described in an earlier paper.[22] The $f \rightarrow f$ transition intensities for $Nd(ClO_4)_3$ in acetonitrile are also included in this table. According to Judd and Jorgensen[29] $f \leftrightarrow f$ transitions which obey $\Delta J = \pm 2$, $\Delta L = \pm 2$ selection rules are the most sensitive to the lanthanide ion environment, and are commonly referred to as hypersensitive. For Nd(III), the $^4I_{9/2} \rightarrow {}^4G_{5/2}$ absorption transition satisfies the above criteria, and, therefore, the intensity of this transition is often used as a probe of structural changes. In practice, the transition $^4I_{9/2} \rightarrow {}^2G_{7/2}$ is very close in energy, and particularly at room temperature, these two transitions must be analyzed together. The absorption transition $^4I_{9/2} \rightarrow {}^4F_{5/2}$ (~802.4 nm) also satisfies partially the selection rule for hypersensitive transitions and is used to monitor structural changes. This transition overlaps with the $^4I_{9/2} \rightarrow {}^2H_{9/2}$ (~794 nm) transition.

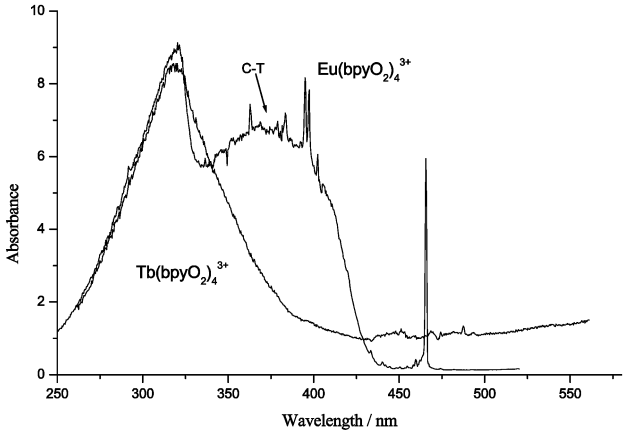

Fig. 3 Excitation spectra of $Tb(bpyO_2)_4(ClO_4)_3$ and $Eu(bpyO_2)_4(ClO_4)_3$ complexes at 77 K ($\lambda_{mon.} = 546.4$ nm for Tb(III) and $\lambda_{mon.} = 612$ nm for Eu(III)).

A comparison of the solid $Nd(bpyO_2)_4(ClO_4)_3$ absorption spectra with those of $Nd(bypO_2)_4^{3+}$ in CH_3CN and CH_3NO_2 illustrates strong similarities between the three systems and significant differences from the results obtained when the complex is dissolved in water.[30,31]

As expected, variations in the structures of the systems under consideration are mainly observed in the spectral range corresponding to the two hypersensitive transitions of Nd(III). The similarity in the results from CH_3CN and CH_3NO_2 is, perhaps not unexpected since the dielectric constants and dipole moments for these solvents are so similar. Similarly, structural modifications caused by the unique properties of aqueous systems, especially in systems in which the ligands are labile, are to be expected. An understanding of the role of solvent, including solvent-induced structural modifications and solvent penetration, is important in studies of complex lability, luminescence efficiency, excited state energetics, and related properties.

We also note that for these non-aqueous systems, the splittings of the $^4I_{9/2} \rightarrow {}^4F_{5/2}, {}^2H_{9/2}$ and the $^4I_{9/2} \rightarrow {}^4F_{7/2}, {}^4S_{3/2}$ transitions in the near-IR are similar, and their intensities as compared to the $^4I_{9/2} \rightarrow {}^4G_{5/2}, {}^2G_{7/2}$ transition are also very similar. Since the solid is known to have a high symmetry from the crystal structure, the similarities suggest a fairly high symmetry environment for the lanthanide ion in these two solutions. It is well known that, for very highly symmetric systems such as O_h and D_{4h}, the intensities of these two transitions in this spectral region are about one half of the intensity of the $^4I_{9/2} \rightarrow {}^4G_{5/2}, {}^2G_{7/2}$ transition[22,32–34] whereas in low symmetry environments, the ratio is significantly higher. In the CH_3CN and CH_3NO_2 solution spectra the ratio of intensities of these transitions is slightly lower than observed for the solid compound. One possible interpretation of these intensity variations is that in solution the ligands are somewhat more able to align themselves in a slightly more symmetric

Table 3 Oscillator strength (*) values for f↔f transitions or integrated intensity for Nd:bpyO$_2$ = 1:4 systems (Judd–Ofelt parameters 10^9, Ω values $\times 10^{20}$)

$^4I_{9/2} \rightarrow S'L'J'$	Wavelength range/nm	$Nd(bpyO_2)_4^{3+}$ in CH_3CN[a]*	$Nd(bpyO_2)_4^{3+}$ in CH_3NO_2[b]*	$Nd(ClO_4)_3$ in CH_3NO_2*	$Nd(bpyO_2)_4(ClO_4)_3$ in paraffin oil	$Nd(bpyO_2)_4(ClO_4)_3$ polycrystal
$^4F_{3/2}$	840–910	335.2	339.5	234.0	20.9	51.25
$^4F_{5/2}$,$^2H_{9/2}$	775–840	975.3	919.2	745.9	71.2	130.63
$^4F_{7/2}$,$^4S_{3/2}$	710–775	678.9	628.5	742.4	44.0	108.3
$^4F_{9/2}$	665–700	60.4	54.6	57.3	2.8	13.8
$^2H_{11/2}$	616–654	13.5	16.8	14.2	1.1	4.2
$^4G_{5/2}$,$^2G_{7/2}$	555–610	7912.2	7162.4	2564.7	400.3	562.1
$^2K_{13/2}$,$^4G_{7/2}$,$^4G_{9/2}$	495–544	1444.0	1395.3	726.7	99.4	179.1
$^2G_{9/2}$,$^2D_{3/2}$,$^4G_{11/2}$,$^2K_{15/2}$	445–495	212.7	186.0	166.3	10.7	33.9
$^2P_{1/2}$,$^2D_{5/2}$	413–440	67.7	65.9	41.2		10.8

[a] $\tau_2 = 3.72$, $\tau_4 = 1.61$, $\tau_6 = 0.68$, $\Omega_2 = 109.01$, $\Omega_4 = 47.18$, $\Omega_6 = 19.82$. [b] $\tau_2 = 3.26$, $\tau_4 = 1.64$, $\tau_6 = 0.61$, $\Omega_2 = 95.66$, $\Omega_4 = 47.99$, $\Omega_6 = 17.84$.

arrangement, since they are free from constraints imposed by crystal packing. This interpretation is consistent with the trends observed from the previously described X-ray structural data, where we noted that in the four ligand molecules, the angles between the ring planes varied because of steric crowding. It should be noted, however, than when the crystals are ground into a powder to produce an isotropic sample, the ratio of the intensities of the discussed three transitions in the spectra of $Nd(bpyO_2)_4(ClO_4)$ is very similar to that observed in solution, indicating that the observed differences discussed above may be due to simple polarization effects in the oriented crystal.

In agreement with previous reports,[30,35] extraordinarily large absorption intensities are observed for the hypersensitive transitions in $Nd(bpyO_2)_4^{3+}$ ($^4I_{9/2} \rightarrow {}^4G_{5/2}$,$^2G_{7/2}$) and $Eu(bpyO_2)_4^{3+}$ ($^7F_0 \rightarrow {}^5D_2$). The integrated intensities are collected in Table 4 for the europium complex. The integrated intensities observed for these complexes and Nd(III) perchlorate dissolved in aqueous solutions are very different.[30,34] As was demonstrated above, in both non-aqueous solvents the $Ln(bpyO_2)_4^{3+}$ species exists predominantly with a structure similar to that in the solid complex. In ref. 1 it was concluded that the structure of $Eu(bpyO_2)_4^{3+}$ possessed D_2 symmetry. From our discussion above, on the basis of X-ray data, it was found that on going from the lanthanum complex (with almost perfect cubic structure) to the neodymium species the symmetry is reduced. The number of observed *SLJ* components [seven for the $^4I_{9/2} \rightarrow {}^4G_{5/2}$,$^2G_{7/2}$ transitions of Nd(III)] corresponds to a symmetry lower than O_h, but is still relatively high.

A careful analysis of the solid neodymium cluster spectra at 4 K shows a number of vibronic components, mainly associated with electronic transitions obeying the $|\Delta J| = 2$ selection rule. According to established theory,[36–38] the vibronic transition probability is described by five terms including the matrix elements of U^2, the unit tensor operator. At 4 K the relative intensities of the three bands ($^4I_{9/2} \rightarrow {}^4G_{5/2}$,$^2G_{7/2}$; $^4F_{5/2}$,$^2H_{9/2}$; $^4F_{7/2}$,$^4S_{3/2}$) are very different from those measured at 300 K, which illustrates the partial vibronic nature of these transitions. Since the calculated values of the individual U^2 matrix elements are drastically different for the above three transitions (0.9736, 0.0102, 0.001), we conclude that the particular vibronic contribution for each of these transitions must also be different.

Table 4 Oscillator strength ($P \times 10^8$) for selected f→f absorption transitions of Eu(III)

Transition	Spectral region/nm	$Eu(bpyO_2)^{3+}$ in CH_3CN	$Eu(bpyO_2)^{3+}$ in CH_3CN	$Eu(ClO_4)_3$ in CH_3CN
$^7F_1 \rightarrow {}^5D_1$	530–542	23.87	25.1	27.1
$^7F_0 \rightarrow {}^5D_1$	524–527	1.8	1.4	1.6
$^7F_0 \rightarrow {}^5D_2$	463–467	94.2	90.2	7.1
$^7F_0 \rightarrow {}^5L_6$[a]	390–410	86.7	82.4	392.1

[a] Transition overlaps with ligand absorption band.

Oscillator strength values, calculated from the electronic spectra of the Nd(III) and Eu(III) samples, are listed in Table 3 and 4. The extraordinarily large intensities for the hypersensitive transitions have led to the use of these high-symmetry complexes as models for the development of theoretical models for f↔f intensity mechanisms. For example, Mason and Stewart[35] interpreted the high intensity of the $^7F_0 \rightarrow {}^5D_2$ transition in $Eu(bpyO_2)_4^{3+}$ acetonitrile solution spectra in terms of a specific contribution associated with a dynamic coupling mechanism. These authors assumed D_4 symmetry for the Eu(III) complex, and showed that an isotropic polarizability of the $bpyO_2$ ligands must be considered in order to account for the large intensity that is observed. Dallara *et al.*[39] have analyzed complexes with trigonal symmetry, and have developed a procedure in which the various contributions of static coupling, and dynamic coupling associated with isotropic and anisotropic ligand polarization, have been determined. In their calculations the Ω_2 intensity parameter is dominated by dynamic-coupling contributions, while $\Omega_4$and Ω_6 parameters by static-coupling ones. Although the calculated and empirically determined correlation between Ω_λ is not perfect, the results of the calculations point at the importance of the dynamic-coupling anisotropy polarizability mechanism contribution in the intensity of the peculiar f–f transitions in the lanthanide systems. Considering our results collected in Table 3 and 4, one can find a very large intensity of the $^4I_{9/2} \rightarrow {}^4G_{5/2}$,$^2G_{7/2}$ transition in the $Nd(bpyO_2)_4^{3+}$ cluster and the $^7F_0 \rightarrow {}^5D_2$ of the europium one, unexpected for relatively highly symmetric systems. Moreover, the observed very large values of Ω_2 parameters manifests that they can be composed of three terms, which are contributions from each of these individual mechanisms: static coupling [SC] and dynamic ones [DC] (isotropic and anisotropic terms). The role of the DC mechanism including anisotropy of the ligand polarizability term in the presented system can explain the extraordinarily large intensity of hypersensitive transitions and Ω_2 parameters. Theoretical calculations of the intensity parameters in the frames of the dynamic-coupling model and basing on X-ray data for our systems can confirm our predictions for the role of anisotropy polarizability of the ligand on the intensity of f–f transitions, especially hypersensitive ones. Such studies are underway.[40]

Excited state energetics of $Tb(bpyO_2)_4^{3+}$

An effort was made to characterize a ligand to metal energy transfer process and the efficiency of terbium emission in the

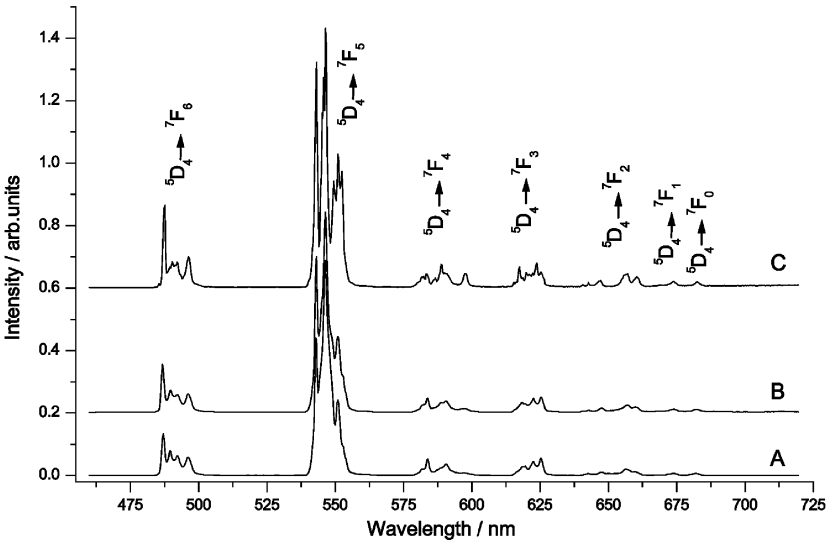

Fig. 4 Luminescence spectra of Tb $(bpyO_2)_4^{3+}$ at 77 K in (A) CH_3CN, (B) CH_3NO_2. The luminescence spectrum of solid $Tb(bpyO_2)_4(ClO_4)_3$ is plotted as (C) ($\lambda_{exc.} = 310$ nm).

solid state and in solution. One interesting aspect of the spectroscopy of the $Tb(bpyO_2)_4^{3+}$ complex is that direct excitation at 293 K of Tb(III) with the intense 488 line of the Ar-ion laser results in undetectable emission in CH_3CN solution at room temperature. One does observe very weak emission from this solution under the same conditions using indirect excitation of the $bpyO_2$ ligand singlet state at 322.5 nm. The 488 nm excitation is also ineffective at inducing emission from solid $Tb(bpyO_2)_4(ClO_4)_3$ and, as above, only weak emission is seen using UV excitation of the ligand. At 77 K luminescence from solid $Tb(bpyO_2)_4(ClO_4)_3$ may be observed under direct and indirect excitation. Observations such as these in other lanthanide complexes[2,4,6,8,41] have been used to determine the effects of various competing excited state processes that are operative in these systems. Lack of emission following direct excitation of Tb(III) in the $bpyO_2$ complex reflects an efficient so-called "back energy transfer" from the metal state to ligand triplet states. There must also exist a forward energy transfer process as shown by the measurement of Tb(III) luminescence at 77 K following ligand singlet excitation. These processes are clearly temperature dependent as shown by the appearance of strong emission from the UV excitation at low temperature, and, obviously, reflect details of the relative location of ligand singlet and triplet states relative to the Tb(III) energy levels.

Emission spectra of $Tb(bpyO_2)_4^{3+}$ in solution and in the solid state at 77 K are presented in Fig. 4. Observed emission bands correspond to transitions from $^5D_4 \rightarrow {}^7F_J$ levels of Tb(III). An analysis of the respective transitions in emission and excitation spectra allows the creation of a Tb(III) energy level diagram as well as the determination of the splitting of the levels. On the other hand, detection of ligand phosphorescence enables one to determine the location of the triplet state. This experiment has been performed with $bpyO_2$ complexes involving Lu(III)[4] and La. The energy of the triplet state has been measured to be 18 349 cm^{-1} using the results for Lu(III),[4] and a similar value, 18 923 cm^{-1}, was obtained using the spectroscopic results for the La(III) complex. These values show that, indeed, the ligand triplet state lies very close and slightly below the Tb(III) $^5D_4$ emitting state, and this is entirely consistent with the observed efficient quenching of Tb(III) emission by the back-energy transfer process.

Additional information concerning the excitation, energy transfer, and de-excitation mechanisms may be obtained by measurement and analysis of excited state lifetimes of Tb(III). Therefore, decay times for $Tb(bpyO_2)_4^{3+}$ in the solid state and in CH_3CN solution were measured at room temperature and 77 K. The results of these measurements are given in Table 5. A comparison of the luminescence spectrum of the solid complex with the frozen solution (77 K) in Fig. 4 confirms the formation of the relatively stable $Tb(bpyO_2)_4^{3+}$ ion in CH_3CN solution. This is the same result observed for the Eu(III) analog.[1] Thus, we assume that emission quenching by multiphonon processes involving solvent vibrations can be neglected. As described below, the excited state processes which are effective in the solid systems and in the solutions are somewhat different. Furthermore, although charge transfer states for Tb(III) can not be considered at the analyzed spectral range (see Fig. 3), the results of the decay measurements show that the mechanism for excited state quenching in $Tb(bpyO_2)_4^{3+}$ systems is not significantly simpler than that observed for $Eu(bpyO_2)_4^{3+}$.

The quantum yield, ϕ_{exp}, of $^5D_4$ emission upon ligand $^1\pi\pi^*$ excitation can be expressed as follows

$$\phi_{exp} = \eta_{et}\eta_r \quad (1)$$

where η_{et} is the energy transfer efficiency from the $^1\pi\pi^*$ state to the $^5D_4$ state of Tb(III), and η_r is luminescence efficiency of $^5D_4$ defined as the ratio of the radiative quenching rate constant, k_r, divided by the sum of the rates of all other processes that deplete the emitting state

$$\eta_r = k_r/\Sigma k \quad (2)$$

If we assume that direct energy transfer from the short-lived $^1\pi\pi^*$ state does not occur, but rather involves an intermediate triplet state [as seems to be the case for many Eu(III) and Tb(III) species], then the energy transfer efficiency may be expressed as

$$\eta_{et} = \eta_{isc}\eta_{et}[^3\pi\pi^*] \quad (3)$$

where η_{isc} is the intersystem crossing efficiency and $[^3\pi\pi^*]$

Table 5 Luminescence lifetimes/ms for Tb(III)

System	τ_{77K}	τ_{300K}
$Tb(bpyO_2)_4(ClO_4)_3$ solid	0.746	0.0418
	0.739	0.01
$Tb(bpyO_2)_4^{3+}$ in CH_3CN solution	0.657	0.003
	0.106	

The decay time curves were not monoexponential both at 77 and 300 K.

denotes the population of the triplet state. Substituting eqn. (3) into eqn. (1) we obtain the following relationship

$$\phi = \eta_{isc}\eta_{et}[^3\pi\pi^*]\eta_r \quad (4)$$

However, in $Tb(bpyO_2)_4^{3+}$ the ligand triplet state is located below the $^5D_4$ state, so use of eqn. (4) is not appropriate. Since we do observe luminescence following excitation of the ligand singlet state, then energy transfer from the $^1\pi\pi^*$ state to higher Tb(III) levels above $^5D_4$ may not be neglected. It also must be the case that the efficiency of energy transfer from ligand singlet state to these higher f-levels (*e.g.* $^5D_3$, $^5D_2$, $^5G_6$) levels must be greater than the back-energy transfer from $^5D_4$ level to the ligand triplet state. Obviously, the fact that no emission can be seen following direct excitation of the complex at room temperature implies that the back-transfer is much more efficient than the formally LaPorte forbidden direct $f \rightarrow f$ absorption process.

Additional insight may be obtained through the decay time measurements. As seen in Table 5, the decay curve for the solid $Tb(bpyO_2)_4^{3+}$ system at 293 K is best fit as a bi-exponential decay with values that differ by more than a factor of 4. At 77 K the decay rate is almost pure mono-exponential since the bi-exponential decay analysis yields values that are virtually identical. In the solids the "back-transfer" rate to the triplet excited state competes with the ligand to metal transfer rate. However at low temperatures, energy transfer leading to $^5D_4$ population is faster than the back-transfer process, and Tb(III) emission is observed. The back energy transfer can be phonon assisted because ΔE between the ligand triplet state and $^5D_4$ of Tb(III) is about 1400 cm^{-1} and it is close to ν(N–O) and ν(ring) stretching vibrations. At higher temperature the reverse is true. Obviously, the back-energy transfer process, which is described by $k_{nr}(T)$, is strongly temperature dependent. The precise source of the temperature dependence of $k_{nr}(T)$ is not obvious from the results so far obtained. The X-ray data show coordination of Tb(III) by oxygen atoms in the N–O groups of $bpyO_2$, however the energy of the N–O vibration modes is not large ($\sim$840, 1280 cm^{-1}),[1,42] and thus quenching by a multiphonon process involving these modes is not very efficient. Clearly, nonradiative processes involving the $bpyO_2$ ligands are temperature dependent. Additional studies involving excited state dynamics of these and other related systems are underway.

4. Summary

The study and analysis of the structures and spectroscopic properties of the complexes of $bpyO_2$ with the series of lanthanide(III) ions has led to useful information in our continuing efforts to understand and derive useful spectra/structure relationships. In particular, the kinds of results presented here should help in the rational design of useful agents exploiting the spin or luminescence properties of lanthanide complexes. Extensions of the work described here aimed at probing the effects of ionic size in the stability of macrocyclic complexes, and a developing a quantitative approach to excited state excitation and de-excitation processes are underway.

Acknowledgements

The authors thank Dr. Zbigniew Ciunik for data collection for $[Lu(bpyO_2)_4](ClO_4)_3$ and cell constants determination for $[Pr(bpyO_2)_4](ClO_4)_3$, $[Ho(bpyO_2)_4](ClO_4)_3$. The production by Dr. Barbara Keller of anhydrous lanthanide perchlorates used in syntheses of the title complexes is also kindly acknowledged. The paper was partially supported by the National Science Foundation of the USA, KBN and Foundation for Polish Science (grant MOLTEK'96).

References

1 (*a*) E. Huskowska, J. Legendziewicz and J. P. Riehl, *International Conference on f-elements (ICFE 3 Paris) Abstracts*, 1997, 256; (*b*) E. Huskowska and J. P. Riehl, *J. Lumin.*, 2000, **86**, 137.
2 P. Gawryszewska, J. Legendziewicz, L. Jerzykiewicz, M. Pietraszkiewicz and J. P. Riehl, *Inorg. Chem.*, 2000, **39**, 5365.
3 P. Gawryszewska, M. Pietraszkiewicz, J. P. Riehl and J. Legendziewicz, *J. Alloys Compd.*, 2000, **300–301**, 283.
4 O. L. Malta, J. Legendziewicz, E. Huskowska, I. Turowska-Tyrk, R. Q. Albuquerque, F. R. G. e Silva and C. De Mello Donega, *J. Alloys Compd.*, 2001, **323–324**, 654.
5 (*a*) J.-M. Lehn., in *Supramolecular Photochemistry*, ed. V. Balzani, Reidel, Dordrecht, The Netherlands, 1987, p. 29; (*b*) L. Prodi, M. Maestri, V. Balzani, J.-M. Lehn and C. Roth, *Chem. Phys. Lett.*, 1991, **180**, 45; (*c*) J.-M. Lehn and C. O. Roth, *Helv. Chim. Acta*, 1991, **74**, 572.
6 N. Sabbatini, M. Guardigli and J.-M. Lehn, *Coord. Chem. Rev.*, 1993, **123**, 201.
7 J. C. G. Bünzli, N. Andre, M. Elhabiri, G. Muller and C. Piguet, *J. Alloys Compd.*, 2000, **303–304**, 66.
8 G. Blasse, G. Dirksen, N. Sabbatini, S. Perathoner, J.-M. Lehn and B. Alpha, *J. Phys. Chem.*, 1988, **92**, 2419.
9 E. Huskowska, P. Gawryszewska, C. L. Maupin, J. Legendziewicz and J. P. Riehl, *J. Alloys Compd.*, 2000, **300–304**, 325.
10 G. F. de Sa, O. L. Malta, C. Mello Donega, A. M. Simas, R. L. Longo, P. A. Santa-Cruz and E. F. da Silva, Jr., *Coord. Chem. Rev.*, 2000, **196**, 165.
11 A. R. Al-Karaghouli, R. O. Day and J. S. Wood, *Inorg. Chem.*, 1978, **17**, 3702.
12 A. R. Al-Karaghouli and J. S. Wood, *J. Chem. Soc., Chem. Commun.*, 1972, 516.
13 W. V. Miller and S. K. Madan, *J. Inorg. Nucl. Chem.*, 1969, **31**, 127.
14 J.-C. Bunzli and J. R. Yersin, *Helv. Chim. Acta*, 1982, **65**, 2498.
15 J. Legendziewicz, G. Oczko, B. Keller, W. Strek and B. Jezowska-Trzebiatowska, *Bull. Acad. Pol. Sci.*, 1984, **32**, 301.
16 W. R. Scheidt and I. Turowska-Tyrk, *Inorg. Chem.*, 1994, **33**, 1314.
17 Kuma KM4CCD Software, version 150, Kuma Diffraction, 1998, Wroclaw, Poland.
18 G. M. Sheldrick, *Acta Crystallogr., Sect. A*, 1990, **46**, 467.
19 G. M. Sheldrick, SHELXL93, Program for the Refinement of Crystal Structures, University of Göttingen, Germany, 1993.
20 G. M. Sheldrick, SHELXL97, Program for the Refinement of Crystal Structures, University of Göttingen, Germany, 1997.
21 H. D. Flack and D. Schwarzenbach, *Acta Crystallogr., Sect. A*, 1998, **44**, 499.
22 J. Legendziewicz, G. Oczko, R. Wiglusz and V. Amirkhanov, *J. Alloys Compd.*, 2001, **323–324**, 792–799.
23 G. B. Drew, *Coord. Chem. Rev.*, 1977, **24**, 179.
24 R. D. Shannon, *Acta Crystallogr., Sect. A*, 1976, **32**, 751.
25 J. Legendziewicz, I. Turowska- Tyrk and M. Borzechowska, to be published.
26 R. Longo, F. R. Goncalves e Silva and Oscar Malta, *Chem. Phys. Lett.*, 2000, **328**, 67.
27 B. R. Judd, *Phys. Rev.*, 1962, **127**, 750.
28 G. S. Ofelt, *J. Chem. Phys.*, 1962, **37**, 511.
29 C. K. Jorgensen and B. R. Judd, *Mol. Phys.*, 1964, **8**, 281.
30 See, for example A. Mesumeci, R. P. Bonomo, V. Cucinotta and A. Seminara, *Inorg. Chim. Acta*, 1982, **59**, 133 and references therein.
31 E. Huskowska, to be published.
32 A. K. Mukhopadhay and M. Chowdury, *Phys. Rev. B*, 1977, **16**, 3070.
33 E. Galdecka, Z. Galdecki, E. Huskowska, V. Amirkhanov and J. Legendziewicz, *J. Alloys Compd.*, 1997, **257**, 182.
34 J. Legendziewicz, *Acta Phys. Pol. A*, 1996, **90**, 127.
35 S. F. Mason and B. S. Stewart, *Mol. Phys.*, 1985, **385**, 611.
36 G. Blasse, *Int. Rev. Phys. Chem.*, 1992, **11**, 71.
37 J. Legendziewicz, *J. Alloys Compd.*, 2000, **300–301**, 71.
38 J. Legendziewicz, G. Oczko and E. Huskowska, *Bull. Acad. Pol. Sci.*, 1984, **42**, 291.
39 J. J. Dallara, M. Reid and F. S. Richardson, *J. Phys. Chem.*, 1984, **88**, 3587.
40 E. Huskowska, J. Legendziewicz and J. P. Riehl, to be published.
41 A. Beeby, D. Parker and J. A. G. Williams, *J. Chem. Soc., Perkin Trans. 2*, 1996, 1565.
42 L. Macalik, J. Hanuza, K. Hermanowicz, W. Ogonowski and H. Ban-Ogonowska, *J. Alloys Compd.*, 2000, **300–301**, 303.